Extension of the Mass Transfer Calculation for Three-Phase Distillation in a Packed Column: Nonequilibrium Model Based Parameter Estimation

Liang Chen,[†] Jens-Uwe Repke,*[,‡] Günter Wozny,[‡] and Shuqing Wang[†]

State Key Lab of Industrial Control Technology, Institute of Cyber-Systems and Control, Zhejiang University, Hangzhou 310027, China, and Institute of Process Engineering, Technische Universität Berlin, 10623 Berlin, Germany

Nonequilibrium (NEQ) modeling of three-phase (vapor−liquid−liquid) distillation in a packed column is still lacking of reliable correlations to calculate the interphase rate-based mass transfer. In this paper, extensions of the two most-used correlations [i.e., the Rocha correlation (Rocha, J. A.; Bravo, J. L.; Fair, J. R. Distillation Columns Containing Structured Packings: A Comprehensive Model for Their Performance. 2. Mass-Transfer Model. *Ind. Eng. Chem. Res.* **1996**, *35*, 1660) and the Billet and Schultes correlation (Billet, R.; Schultes, M. Prediction of Mass Transfer Columns with Dumped and Arranged Packings: Updated Summary of the Calculation Method of Billet & Schultes. *Chem. Eng. Res. Des.* **1999**, *77*, 498)] are proposed for mass transfer calculation of three-phase distillation in a packed column. Parameters used in the correlations are estimated on the basis of comprehensive experimental investigations on both two-phase (vapor−liquid) and three-phase distillation. The experimental database contains 150 different experiments of the 1-butanol/water/1-propanol system for different packings (Montz-Pak B1-350, Raschig Super-Ring 0.3, Rombopak 9M). The parameter estimation with multiple data sets and multipacking turns out to be a large-scale optimization problem subjected to a large number of nonlinear model equations. To reduce the problem dimension and remove coupling among the parameters, a hierarchical estimation strategy is proposed. The parameters are classified into packing-related and flow-related parameters, which are estimated using two-phase and three-phase distillation experimental data, respectively. In this way, the extension of mass transfer calculation for three-phase distillation is derived. Substantial improvements in the NEQ model prediction have been achieved. Compared with two-phase distillation, an increase of overall mass transfer ability is observed for the studied three-phase system. The extension of the mass transfer calculation can give a reasonable explanation for this observation, providing a better understanding of the intrinsic transfer phenomena inside three-phase packed columns.

1. Introduction

Multicomponent and multiphase distillations are common separation processes in the chemical and petroleum industry. There are many examples of extractive and azeotropic distillation processes, in which binary azeotropes are broken by adding a third component that creates a vapor−liquid−liquid (three-phase) distillation.[1] Modeling three-phase distillation in a packed column, however, is a vague and complicated task due to the strong influence of the second liquid on the mass and heat transfer. It is difficult to accurately describe the fluid dynamic behaviors of two immiscible liquid phases inside the packed distillation column.

When three-phase distillation processes are modeled, both the equilibrium (EQ) and the nonequilibrium (NEQ, or rate-based) approaches are available. The EQ approach can be traced back to as early as the 1970s, when Block and Hegner[2] first proposed a simulation model for three-phase distillation. The three-phase NEQ model, however, did not appear in the literature until the 1990s.[3] Compared with the EQ model, the three-phase NEQ model is more rigorous and avoids using the empirical Murphree efficiency (tray column) or HETP value (packed column), which are quite unreliable for multicomponent and multiphase systems.[3,4] Cairns and Furzer[5] explicitly warned against incorporating the Murphree efficiency into the simulation model for three-phase systems. Some distinct phenomena of three-phase distillation cannot be described by using the EQ model.[4,9,11] The NEQ model, dominated by the fundamental mass and heat transfer equations,[6] is certainly more complex in nature and superior in theory for tray columns[1,6−9] and for packed columns.[10−12] The key concept of the NEQ model is the direct calculation of the rate-based interphase mass transfer, which is frequently described as[1,3,4,6,8,11,13]

$$\mathbf{J} = -c_t[\mathbf{k}]\nabla\mathbf{z} = c_t[\mathbf{B}]^{-1}[\mathbf{\Gamma}](\mathbf{z}^{\mathbf{I}} - \mathbf{z}) \tag{1}$$

where the thermodynamic matrix $[\mathbf{\Gamma}]$ can be derived from a certain activity coefficient model (NRTL, UNIQUAC, etc.) and the $[\mathbf{B}]$ matrix has the elements

$$B_{ij} = -z_i\left(\frac{1}{\beta_{ij}} - \frac{1}{\beta_{in}}\right) \quad \text{and} \quad B_{ii} = \frac{z_i}{\beta_{in}} + \sum_{k=1(i\neq k)}^{n}\frac{z_k}{\beta_{ik}} \quad [i, j = 1, ..., n-1\ (i \neq j)] \tag{2}$$

Unfortunately, for multicomponent distillation, there is no theoretical method dedicated to compute the binary mass transfer coefficient β in eq 2. Alternatively, empirical mass transfer correlations have been developed to tackle the problem. For packed columns, one early and still widely used correlation to describe vapor/liquid mass transfer was developed by Onda and co-workers.[14] Shi and Mersmann[15] lately proposed a more rigorous correlation based on the fluid dynamics of rivulet flow.

* To whom correspondence should be addressed. E-mail: Jens-Uwe.Repke@TU-Berlin.DE.
[†] Zhejiang University.
[‡] Technische Universität Berlin.

10.1021/ie900404p CCC: $40.75
Published on Web 06/10/2009

Table 1. Most-Used Mass Transfer Correlations for a Packed Column

correlation	β^V, β^L, a_e	comments
Rocha (SRP II)[17,18]	$\frac{a_e}{a_p} = F_{SE}\frac{29.12 d_h^{0.359}(Re_L)^{\theta_1}(We_L)^{\theta_2}(Fr_L)^{\theta_3}}{\varepsilon^{0.6}(1 - 0.93\cos\gamma)(\sin\eta)^{0.3}}$	for structured packings
	$\beta^V = 0.054 D_V/d_h (Re_V)^{\theta_4}(Sc_V)^{\theta_5}$	
	$\beta^L = 2\sqrt{\frac{D_L}{\pi t_{res}}} = 2\sqrt{\frac{C_E D_L}{\pi d_h}}\left(\frac{u_L}{\varepsilon h_L \sin\eta}\right)^{\theta_6}$	
Billet and Schultes[19,a]	$\frac{a_e}{a_p} = 1.5\frac{1}{\sqrt{a_p d_h}}(Re_L)^{\theta_1}(We_L)^{\theta_2}(Fr_L)^{\theta_3}$	for both random and structured packings, up to the flooding point
	$\beta^V = C_V\sqrt{\frac{a_p}{(\varepsilon - h_L)d_h}} D_V (Re_V)^{\theta_4}(Sc_V)^{\theta_5}$	
	$\beta^L = 1.514 C_L\sqrt{\frac{D_L}{d_h}}\left(\frac{u_L}{h_L}\right)^{\theta_6}$	

[a] An extension of the Billet and Schultes correlation for operations between the loading point and flooding point is given in ref 19.

However, these correlations can only be applied to random packings. The first overall investigation about structured (gauze) packing was conducted by Bravo and co-workers.[16] The results were called the SRP I model, which has recently been improved and updated by Rocha et al.,[17,18] i.e., the SRP II model. A significant characteristic of the SRP II model is that the mass transfer and hydraulic performance of structured packing are related by liquid holdup. Billet and Schultes[19] also mentioned this point in their study. They developed an advanced empirical model for mass transfer calculation in a vapor−liquid countercurrent column, filled with either random or structured packings, in the entire loading range. There are also other mass transfer models (e.g., the Delft model[20]) existing for two-phase packed distillation. A comprehensive review on mass transfer correlations for a packed column[21] is available. To the our best knowledge, the Rocha correlation and Billet and Schultes correlation are the two most-used correlations for packed distillation and have been revised or extended for different applications.[21] The formulations of both correlations are given in Table 1.

The above correlations were originally developed for vapor−liquid (two-phase) distillations (and absorptions). For three-phase distillation in a packed column, unfortunately, no mass transfer correlation can be found in the literature. The motivation of this paper is to propose extensions of mass transfer correlations (to be accurate, extensions of an applicable range of correlations, abbreviated as "extended correlation", the same hereinafter) for three-phase packed distillation. As a result, the extensions of mass transfer correlations (Rocha correlation, Billet and Schultes correlation) are derived on the basis of parameter estimation. The main idea is to formulate a multiple-data-set optimization problem to estimate a set of parameters used in the correlation to minimize the deviations between simulations and experiments. The simulation was performed on the basis of a rigorous NEQ three-phase distillation model presented in section 2. The experiments were carried out in a laboratory-scale packed column and contain comprehensive investigations on two-phase and three-phase distillations. Details about the experimental setup and the available database are given in section 3. In the estimation, parameters in the correlation are classified into packing-related parameters and flow-related parameters, which are estimated using two-phase and three-phase distillation data sets, respectively. This strategy, called hierarchical parameter estimation, is described in section 3. In section 4, an extension of the Billet and Schultes correlation is carried out as an illustrative example. Substantial improvements in the simulation predictive ability are observed by applying the NEQ model with the extended correlations. Furthermore, the extension of mass transfer calculation could provide more insights into three-phase transfer phenomena as revealed in section 5.

2. Nonequilibrium Modeling

The flow behavior of three-phase packed distillation has been investigated via experiments and CFD (computational fluid dynamics) simulations.[22,27,29−32]

Complex and extraordinary fluid dynamics is observed. On a three-phase packing element, two immiscible liquid phases flow down cocurrently and the vapor phase flows up countercurrently. The continued liquid phase (i.e., the first liquid) forms a closed film on the packing surface, while the dispersed liquid phase (i.e., the second liquid) forms rivulets and droplets.[22,20−31] Moreover, the second liquid could flow either above or below the first liquid film and change the effective interfacial areas and vapor-side and liquid-side mass transfer in a dramatic way.[30−32]

A schematic representation of a three-phase packing section is depicted in Figure 1. For simulation, the packed column is divided into several such sections. In contrast to the EQ model,

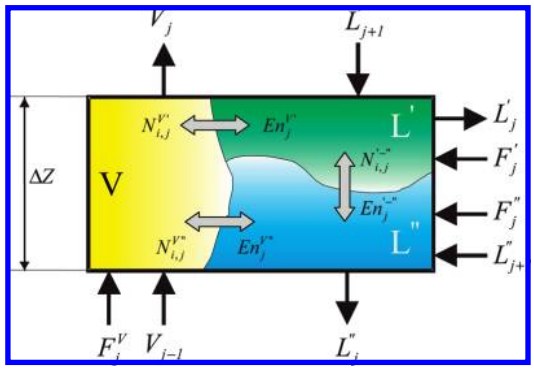

Figure 1. Schematic diagram of a three-phase packing section. Reprinted with permission from ref 11. Copyright 2004 Elsevier.

the material and energy balances in the NEQ model are formulated for each individual phase (vapor phase, V; first liquid phase, L′; second liquid phase, L″) rather than the whole section. The basic idea of the NEQ model is the explicit consideration of mass and heat transfer from one phase to another. In the three-phase NEQ model, mass and energy transfer occurs among all three phases, and equilibrium is only considered at the phase interface. Each phase is linked and influenced by the mass transfer flux $N_{i,j}$ and energy transfer rates $E_{n,j}$ from the other two phases. Here, $N^{V'}_{i,j}$ is, for example, the molar flux of component i in section j from the vapor phase to the first liquid phase. The mathematical equations of the NEQ model for a three-phase packing section are summarized in Table 2.

The main uncertainty of the three-phase NEQ model is the absence of applicable correlations to calculate the binary mass transfer coefficients $\beta^{V'}$, β'^{V}, $\beta^{V''}$, β''^{V}, $\beta'^{-''}$, and $\beta''^{-'}$ and the effective interfacial areas $a^{V'}$, $a^{V''}$, and $a'^{-''}$. Most previous publications on three-phase modeling had to use the correlations,[14−21] which are only validated for two-phase distillation. These correlations may be used as starting points, yet for more rigorous modeling of three-phase distillation, they should be adapted according to the hydrodynamics of three-phase distillations.

In the three-phase NEQ model, the binary mass transfer coefficients are computed separately for each interface from both the vapor and liquid sides. Here, the Billet and Schultes correlation is used.

$$\beta^{V'} = C_V \sqrt{\frac{a_p}{(\varepsilon - h_{L'})d_h}} D_V (Re_V)^{\theta_4} (Sc_V)^{\theta_5} \quad (3)$$

$$\beta^{V''} = C_V \sqrt{\frac{a_p}{(\varepsilon - h_{L''})d_h}} D_V (Re_V)^{\theta_4} (Sc_V)^{\theta_5} \quad (4)$$

$$\beta'^{V} = 1.154 C_L \sqrt{\frac{D_{L'}}{d_h}} \left(\frac{u_{L'}}{h_{L'}}\right)^{\theta_6} \quad (5)$$

$$\beta''^{V} = 1.154 C_L \sqrt{\frac{D_{L''}}{d_h}} \left(\frac{u_{L''}}{h_{L''}}\right)^{\theta_6} \quad (6)$$

The total effective interfacial area a_e is calculated using the average properties of two liquids, i.e., $\bar{R}e_L$, $\bar{W}e_L$, and $\bar{F}r_L$

$$\frac{a_e}{a_p} = 1.5 \frac{1}{\sqrt{a_p d_h}} (\overline{Re}_L)^{\theta_1} (\overline{We}_L)^{\theta_2} (\overline{Fr}_L)^{\theta_3} \quad (7)$$

and then distributed according to the volumetric ratios of each liquid (φ' and φ'', respectively)[12]

$$a^{V'} = \varphi' a_e \quad (8)$$

$$a^{V''} = \varphi'' a_e \quad (9)$$

In the correlation eqs 3−9, the parameters [C_V, C_L] and [θ_1, θ_2, ..., θ_6] remain unknown for three-phase distillation. They have to be estimated on the basis of the experimental database for extension of mass transfer calculation in three-phase distillation. For the liquid−liquid interface, the binary mass transfer coefficients $\beta'^{-''}$ and $\beta''^{-'}$ are computed by the method of a laminar falling film;[12,13] i.e., $\beta'^{-''} = D_{L'}/\delta_{L'}$ and $\beta''^{-'} = D_{L''}/\delta_{L''}$. For the effective interfacial area, it is assumed $a'^{-''} = a^{V''}$. Previous studies on three-phase NEQ modeling usually assumed a liquid−liquid equilibrium,[7,9,10] which means that $\beta'^{-''}$, $\beta''^{-'}$, and $a'^{-''}$ are not crucial to the overall mass transfer. This conclusion is also validated in this study (see section 5, Figure 10). Therefore, the extensions of mass transfer calculation for $\beta'^{-''}$, $\beta''^{-'}$, and $a'^{-''}$ are not considered in this paper.

The three-phase NEQ model consists of a large number of variables and nonlinear equations. Degree of freedom analysis shows that there are a total of $21C^2 - 12C + 30$ equations and variables for each NEQ packing section, which contains $12C + 9$ primary variables and equations.[1,3,12] A summary of the variables and equations is given in Table 3. It is notable that the number of transfer variables ($21C^2 - 24C + 21$) is much more than that of primary variables ($12C + 9$). Taking a ternary system, for example, around 75−80% of the variables and equations are used to compute the transfer variables. Compared with the three-phase EQ model, the NEQ model is more rigorous in principle, meanwhile more complex in model equations. If the second liquid does not appear, the above model reduces to the two-phase NEQ model, a special case of the three-phase NEQ model. It is easy to verify that the two-phase NEQ model is a system with $8C^2 - 3C + 11$ variables and equations.

It is worth noting that a phase stability check is not considered in the three-phase simulations, because the special experiment designs can guarantee pure two-phase distillations and pure three-phase distillations; i.e., no transition from two phases to three phases happened between the packing sections.

3. Parameter Estimation Problem

3.1. Experimental Database. As shown in Figure 2 (left), a laboratory-scale packed column was built up in the Institute of Process Engineering (TU Berlin) to produce a representative experimental database of three-phase distillation for parameter estimation. The column has an inner diameter of 0.1 m and a whole height of 6.2 m. The maximum packing height is 2.4 m. The column consists of a thermosiphon reboiler (with a forced recirculation pump). The maximum heat duty of the reboiler is up to 30 kW, and the corresponding maximum F-factor (defined as $U_V \rho_V^{1/2}$) is up to 3.0 $Pa^{0.5}$. By means of a process control system, the operational variables such as the pressure drop, temperature, cooling water flow rate, and reflux flow rate are measured and controlled. The liquid loads in the column during the experiments are between 0.5 and 40 $m^3/(m^2 \cdot h)$. More information about the experimental setup is listed in Table 4.

Extensive investigations, consisting of around 150 different experiments for both two-phase and three-phase distillations, were carried out. The studied component mixture system was 1-butanol/water/1-propanol. The system contains two binary azeotropes (one homogeneous, one heterogeneous), and it has a relatively small miscibility gap shown in Figure 2 (right), indicating a limited range of concentration in three-phase distillations. Both open and closed structured packing and

Table 2. NEQ Model Equations for Three-Phase Distillation in a Packed Column

Component material balance for each phase

$$F_j^V y_{i,j}^F + V_{j-1} y_{i,j-1} - V_j y_{i,j} - \left(N_{i,j}^{V'}\right) a_j^{V'} - \left(N_{i,j}^{V''}\right) a_j^{V''} = 0$$

$$F_j' x_{i,j}^{F'} + L_{j+1}' x_{i,j+1}' - L_j' x_{i,j}' + \left(N_{i,j}^{V'}\right) a_j^{V'} - \left(N_{i,j}^{L'-''}\right) a_j^{L'-''} = 0$$

$$F_j'' x_{i,j}^{F''} + L_{j+1}'' x_{i,j+1}'' - L_j'' x_{i,j}'' + \left(N_{i,j}^{V''}\right) a_j^{V''} + \left(N_{i,j}^{L'-''}\right) a_j^{L'-''} = 0$$

Heat balances for each phase

$$F_j^V H_j^F - V_j H_j^V + V_{j-1} H_{j-1}^V - En_j^{V'} - En_j^{V''} + Q_j^V = 0$$

$$F_j' H_j^{F'} - L_j' H_j' + L_{j+1}' H_{j+1}' + En_j^{V'} - En_j^{L'-''} + Q_j' = 0$$

$$F_j'' H_j^{F''} - L_j'' H_j'' + L_{j+1}'' H_{j+1}'' + En_j^{V''} + En_j^{L'-''} + Q_j'' = 0$$

Bulk phase mole fraction summations

$$\sum_{i=1}^{n} y_{i,j} = 1, \quad \sum_{i=1}^{n} x_{i,j}' = 1, \quad \sum_{i=1}^{n} x_{i,j}'' = 1$$

Interface equilibrium

$$y_{i,j}^{V'} = K_{i,j}^{V'} x_{i,j}^{\overline{V}}, \quad y_{i,j}^{V''} = K_{i,j}^{V''} x_{i,j}^{\overline{V}}, \quad x_{i,j}^{L'-''} = K_{i,j}^{L'-''} x_{i,j}^{L''-'}$$

Interface mole fraction summations

$$\sum_{i=1}^{n} y_{i,j}^{V'} = 1, \quad \sum_{i=1}^{n} x_{i,j}^{\overline{V}} = 1, \quad \sum_{i=1}^{n} y_{i,j}^{V''} = 1,$$

$$\sum_{i=1}^{n} x_{i,j}^{\overline{V}} = 1, \quad \sum_{i=1}^{n} x_{i,j}^{\overline{L'-''}} = 1, \quad \sum_{i=1}^{n} x_{i,j}^{\overline{L''-'}} = 1$$

Mass transfer coefficient matrix calculation

$$[k^V] = [B^V]^{-1}[\Xi^V], \quad [k^L] = [B^L]^{-1}[\Gamma][\Xi^L]$$

$$B_{ii} = \frac{z_i}{\beta_{in}} + \sum_{\substack{k=1 \\ i \neq k}}^{n} \frac{z_k}{\beta_{ik}} \quad \text{and} \quad B_{ij} = -z_i\left(\frac{1}{\beta_{ij}} - \frac{1}{\beta_{in}}\right)$$

Mass transfer flux equations

V-L′ Interface

$$N_{i,j}^{V'} = \overline{C}_j^{V} \sum_{m=1}^{n-1}\left(k_{i,m,j}^{V'}\left(\overline{y}_{m,j}^{V} - y_{m,j}^{V'}\right)\right) + \overline{y}_{i,j}^{V} \sum_{i=1}^{n} N_{i,j}^{V'}$$

$$N_{i,j}^{V'} = \overline{C}_j' \sum_{m=1}^{n-1}\left(k_{i,m,j}^{\overline{V}}\left(x_{m,j}^{\overline{V}} - \overline{x}_{m,j}'\right)\right) + \overline{x}_{i,j}' \sum_{i=1}^{n} N_{i,j}^{V'}$$

V-L″ Interface

$$N_{i,j}^{V''} = \overline{C}_j^{V} \sum_{m=1}^{n-1}\left(k_{i,m,j}^{V''}\left(\overline{y}_{m,j}^{V} - y_{m,j}^{V''}\right)\right) + \overline{y}_{i,j}^{V} \sum_{i=1}^{n} N_{i,j}^{V''}$$

$$N_{i,j}^{V''} = \overline{C}_j'' \sum_{m=1}^{n-1}\left(k_{i,m,j}^{\overline{V}}\left(x_{m,j}^{\overline{V}} - \overline{x}_{m,j}''\right)\right) + \overline{x}_{i,j}'' \sum_{i=1}^{n} N_{i,j}^{V''}$$

L′-L″ Interface

$$N_{i,j}^{L'-''} = \overline{C}_j^{-} \sum_{m=1}^{n-1}\left(k_{i,m,j}^{L'-''}\left(\overline{x}_{m,j}^{-} - x_{m,j}^{L'-''}\right)\right) + \overline{x}_{i,j}^{-} \sum_{i=1}^{n} N_{i,j}^{L'-''}$$

$$N_{i,j}^{L'-''} = \overline{C}_j'' \sum_{m=1}^{n-1}\left(k_{i,m,j}^{L''-'}\left(x_{m,j}^{L''-'} - \overline{x}_{m,j}''\right)\right) + \overline{x}_{i,j}'' \sum_{i=1}^{n} N_{i,j}^{L'-''}$$

Energy transfer rate equations

V-L′ Interface

$$En_j^{V'} = \left(\alpha_j^{V'}\left(\overline{T}_j^{V} - T_j^{V'}\right) + \sum_{i=1}^{n}\left(N_{i,j}^{V'} \overline{H}_{i,j}^{V}\right)\right) a_j^{V'}$$

$$En_j^{\overline{V}} = \left(\alpha_j^{\overline{V}}\left(T_j^{V'} - \overline{T}_j'\right) + \sum_{i=1}^{n}\left(N_{i,j}^{\overline{V}} \overline{H}_{i,j}'\right)\right) a_j^{V'}$$

V-L″ Interface

$$En_j^{V''} = \left(\alpha_j^{V''}\left(\overline{T}_j^{V} - T_j^{V''}\right) + \sum_{i=1}^{n}\left(N_{i,j}^{V''} \overline{H}_{i,j}^{V}\right)\right) a_j^{V''}$$

$$En_j^{\overline{V}} = \left(\alpha_j^{\overline{V}}\left(T_j^{V''} - \overline{T}_j''\right) + \sum_{i=1}^{n}\left(N_{i,j}^{\overline{V}} \overline{H}_{i,j}''\right)\right) a_j^{V''}$$

L′-L″ Interface

$$En_j^{L'-''} = \left(\alpha_j^{L'-''}\left(\overline{T}_j' - T_j^{L'-''}\right) + \sum_{i=1}^{n}\left(N_{i,j}^{L'-''} \overline{H}_{i,j}'\right)\right) a_j^{L'-''}$$

$$En_j^{\overline{L''-'}} = \left(\alpha_j^{L''-'}\left(T_j^{L'-''} - \overline{T}_j''\right) + \sum_{i=1}^{n}\left(N_{i,j}^{\overline{L''-'}} \overline{H}_{i,j}''\right)\right) a_j^{L'-''}$$

Where

$$\overline{T}_j^{V} = \frac{T_{j-1}^{V} + T_j^{V}}{2}, \quad \overline{T}_j' = \frac{T_j' + T_{j+1}'}{2}, \quad \overline{T}_j'' = \frac{T_j'' + T_{j+1}''}{2}, \quad \overline{y}_{m,j}^{V} = \frac{y_{m,j-1}^{V} + y_{m,j}^{V}}{2}, \quad \overline{x}_{m,j}' = \frac{x_{m,j}' + x_{m,j+1}'}{2}, \quad \overline{x}_{m,j}'' = \frac{x_{m,j}'' + x_{m,j+1}''}{2}$$

$$\overline{C}_j^{V} = \frac{P}{R\overline{T}_j^{V}}, \quad \overline{C}_j' = \left(\sum_{i=1}^{n}\left(\frac{\overline{x}_{i,j}' M_i}{\rho_{i,j}}\right)\right)^{-1}, \quad \overline{C}_j'' = \left(\sum_{i=1}^{n}\left(\frac{\overline{x}_{i,j}'' M_i}{\rho_{i,j}}\right)\right)^{-1}$$

Table 3. Number of Equations and Variables in the Three-Phase NEQ Model

equation	number	variable	number
primary equations	$12C + 9$	primary variables	$12C + 9$
component material balance for each phase	$3C$	vapor and liquid flows V, L', L''	3
heat balances for each phase	3	mole fraction for each phase y, x', x''	$3C$
bulk phase mole fraction summations	3	interface mole fractions $y^{V'}$, $y^{V''}$, x^{V},$x^{L'-''}$, $x^{L''-'}$	$6C$
interface equilibrium	$3C$	mass transfer rates $N^{V'}$, $N^{V''}$, $N^{L'-''}$	$3C$
interface mole fraction summations	6	heat transfer rates $E_n^{V'}$, $E_n^{V''}$, $E_n^{L'-''}$, E_n^{V}, $E_n^{L''-'}$, $E_n^{L''-'}$	6
heat transfer equations	3	temperature of each phase T^{V}, T',T''	3
mass transfer equations	$6(C-1)$	temperatures at the interfaces $T^{V'}$, $T^{V''}$, $T^{L'-''}$	3
transfer equations	$21C^2 - 24C + 21$	transfer variables	$21C^2 - 24C + 21$
Fuller equation[13] to calculate D_V	C^2	binary diffusion coefficients D_V, D_L	$3C^2$
Vignes equation[13] to calculate D_L	$2C^2$	binary mass transfer coefficient β	$6C^2$
Billet and Schultes or Rocha correlation	$4C^2 + 3$	inverted mass transfer matrix [**B**]	$6(C-1)^2$
falling film method	$2C^2$	multicomponent mass transfer coefficient [**k**]	$6(C-1)^2$
mass transfer coefficient matrix calculation	$12(C-1)^2$	effective interfacial areas$a^{V'}$, $a^{V''}$, $a^{L'-''}$	3
Chilton−Colburn[13,22] analogy	6	heat transfer coefficient α	6
total equations	$21C^2 - 12C + 30$	total variables	$21C^2 - 12C + 30$

random packing were investigated to consider all potential possibilities of three-phase distillations. The *F*-factor was used as an indicator of the hydrodynamic state of the internal flows and to characterize the operation conditions. The detailed *F*-factor ranges for two-phase and three-phase distillations are given in Table 4.

Concentration measurements were sampled along the column and used as the basic data sets for model validation and parameter estimation. Four vapor and four liquid samples were taken from suitable locations (see Figure 2) of the column. The samples below and above the packing section are of great importance, since they directly reflect the mass transfer ability. Due to the potential possibility of two coexisting liquids, all samples were first dissolved into a reference solvent, ethanol, before injection into the gas chromatograph. Each sample was analyzed by gas chromatography three times, and the average

Table 4. Experiment Details

	system setup	remarks
packing	Montz-Pak B1-350	type: closed structured
	Rombopak 9M	type: open structured
	Raschig Super-Ring 0.3	type: ring random
component	1-butanol/water/1-propanol	small miscibility gap
experiment	two-phase distillation	F-factor 0.16−2.55 $Pa^{0.5}$
	three-phase distillation	F-factor 1.01−2.68 $Pa^{0.5}$
condenser	total condenser, total reflux	
reboiler	maximum 30 kW (F-factor up to 3.0 $Pa^{0.5}$)	

value was regarded as the concentration of the vapor or liquid phase. More details can be found in our previous papers.[23−25]

3.2. Hierarchical Estimation Strategy. It is difficult to derive a theoretical mass transfer correlation for three-phase packed distillation because there are so many factors that may contribute to the vapor−liquid−liquid mass transfer.

First, the packing used in the column has a direct impact on the mass transfer ability. These packing-related factors include the geometry (ring, saddle, gauze, sheet), material (metal, ceramic, plastic), specific packing area, void fraction, corrugation angle, etc.

Second, the appearance of the second liquid will introduce an additional influence on the interphase mass transfer. There is abundant evidence[22,29−32] of the unique flow behaviors caused by the second liquid; e.g., film breakup and rivulet flow (or droplet flow) were observed in experimental[22,29] and CFD[30−32] investigations. The flow-related factors such as the superficial velocities, liquid holdups, film thickness, physical properties, interfacial area, etc. will be changed as the second liquid appears.

It is too complicated to consider all the above factors in a three-phase mass transfer correlation. An extension of the existing two-phase correlation may be the first step toward deriving a reliable correlation for three-phase packed distillation. Several successful correlations for a two-phase packed column are available.[17−19,21] A common characteristic of these correlations is the use of the so-called packing-related parameters[15,18,19] to emphasize the difference in mass transfer ability provided by different packings; i.e., packing-related parameters (e.g., C_V and C_L in the Billet and Schultes correlation and F_{SE} in the Rocha correlation) are used to represent the overall effect of the packing-related factors on the mass transfer. These parameters are usually assumed to be constants, which are only linked with the packing styles.[17−19] Concerning three-phase distillation, the change of flow behaviors will be reflected in the Reynolds number (Re_L, Re_V), Weber number (We_L), Froude number (Fr_L), Schmidt number (Sc_V), etc. in the correlation (see eqs 3−9). Therefore, it would be reasonable to change (or re-estimate) the exponential parameters [θ_1, ..., θ_6] related to these terms; i.e., flow-related parameters (defined as [θ_1, θ_2, θ_3, ..., θ_6] in Table 1) reflect directly the influence of the flow behavior changed by the second liquid in this work. This represents the main idea of correlation extension.

It is worth noting, however, packing-related parameters and flow-related parameters are inherently linked. The term "packing-related" is inherited from previous papers,[17−19] while the term "flow-related" is used to isolate the hydrodynamic effect of the second liquid and only represents the overall influence of the second liquid on the mass transfer.

For some newly released packings, the values of the packing-related parameters are not available. Therefore, a preliminary estimation of the packing-related parameters using two-phase experiments is needed. In a later step, the flow-related parameters can be estimated on the basis of three-phase experiments. This is the so-called hierarchical estimation strategy in this paper.

To make this strategy applicable, a special design of the experiments is required. Concerning the experiments described in the previous section, the corresponding two-phase and three-phase distillations are carried out using the same column

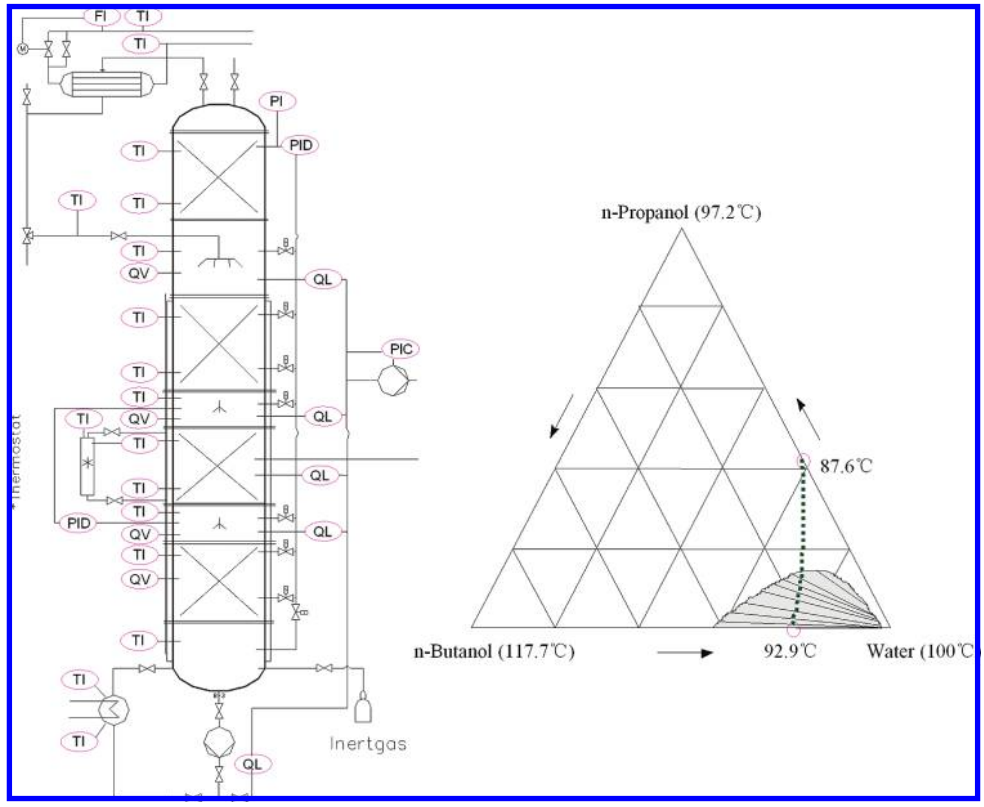

Figure 2. Left: experiment setup of the packed column. Right: triangle phase diagram.

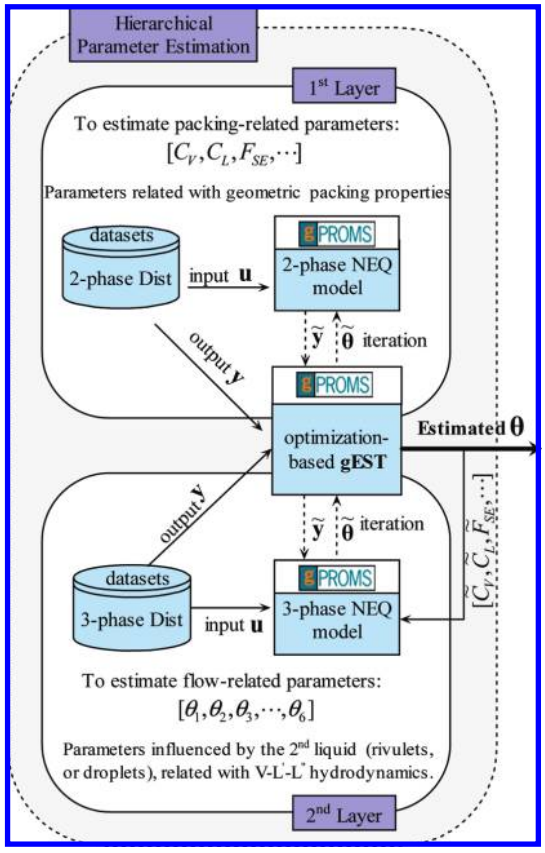

Figure 3. Flow sheet of hierarchical parameter estimation.

equipped with the same packing and similar operation conditions to isolate the influence of the second liquid as best as one can.

The hierarchical (or two-layer) estimation strategy is illustrated in Figure 3. The packing-related parameters are assumed to be identical for two-phase and three-phase distillation. Hence, two-phase experimental data are utilized to estimate the packing-related parameters in the first-layer estimation. It is notable that the exponential parameters [θ_1, θ_2, θ_3, ..., θ_6] are fixed to the original values, while C_V, C_L, and F_{SE} are estimated and differ from packing to packing. The estimated packing-related parameters C_V, C_L, and F_{SE} are then passed into the second layer as given values to estimate the exponential flow-related parameters [θ_1, θ_2, θ_3, ..., θ_6]. These parameters are considered packing-independent and only account for the special hydrodynamics of three-phase distillation itself. They are estimated on the basis of experimental data sets of three-phase distillation. Therefore, the original estimation problem is reduced into several subestimation problems, while the accuracy of the estimated parameters would be guaranteed by the strategy.

The parameter estimations are carried out in gPROMS. The NEQ models of two-phase and three-phase distillation described in section 2 are built up for simulation. The mass transfer correlations in Table 1 are used for the rate-based mass transfer calculation. The gEST entity is used to integrate the NEQ model and experimental database and to minimize the deviations between them. The detailed mathematical formulation of the NEQ model based parameter estimation is discussed in the next section.

3.3. Mathematical Formulation. The approach of principle model based parameter estimation may be difficult, since the thermophysical properties and phase equilibrium calculation are inherently linked with the objective function. However, it is available nowadays due to the fast development of computational ability.[33−36]

The main idea of the parameter estimation is to formulate a multiple-data-set optimization problem subjected to the NEQ model equation. A general parameter estimation problem with multiple data sets is formulated as

$$\Phi(\boldsymbol{\theta}) = \frac{N}{2}\ln(2\pi) + \frac{1}{2}\min_{\boldsymbol{\theta}} \sum_{i=1}^{\mathrm{NDS}} [\sum_{j=1}^{\mathrm{NV}} \ln(\omega_{i,j}^{\ 2}) + (\mathbf{y}_i - \tilde{\mathbf{y}}_i)^T \boldsymbol{\omega}_i^{-1} (\mathbf{y}_i - \tilde{\mathbf{y}}_i)] \quad (10)$$

subject to

$$\mathbf{g}_i(\mathbf{x}_i, \mathbf{y}_i, \mathbf{u}_i, \boldsymbol{\theta}) = 0$$

$$\mathbf{h}_i(\mathbf{x}_i, \mathbf{y}_i, \mathbf{u}_i, \boldsymbol{\theta}) \geq 0 \quad i = 1, ..., \mathrm{NDS}$$

$$\boldsymbol{\theta}^{\mathrm{L}} \leq \boldsymbol{\theta} \leq \boldsymbol{\theta}^{\mathrm{U}}$$

N = total number of measurements [N = (NDS)(NV)], NDS = number of data sets, and NV = number of variables measured in each experiment. To estimate the parameters $\boldsymbol{\theta}$ in a nonlinear implicit equation system, there are normally several experimental data sets of output variables $\mathbf{y}$ ($\tilde{\mathbf{y}}$, simulation prediction) and the input (manipulated) variables $\mathbf{u}$. There are also many unmeasurable state variables $\mathbf{x}$ in the model equations $\mathbf{g}$ and inequality constraints $\mathbf{h}$. In this study, we assume the output variables $\mathbf{y}$ are subjected to measurement error, while the manipulated variables $\mathbf{u}$ are free of error (i.e., only the covariance matrix $\boldsymbol{\omega}$ of output variables was considered in the maximum likelihood objective function $\boldsymbol{\Phi}$). Therefore, a more complicated errors-in-variables (EVM) parameter estimation problem is avoided.[26]

Considering the proposed hierarchical parameter estimation, here

Table 5. Problem Dimension Analysis

	objective	model	packing	NDS	problem dimension[a]	
first-layer estimation	packing-related parameters	two-phase NEQ model	Montz-Pak B1−350	10	(NDS)($8C^2 - 3C + 11$)(NP) + P_1 =	2962
			Rombopak 9M	12		3554
			Super-Ring 0.3	16		4738
second-layer estimation	flow-related parameters	three-phase NEQ model	all packings	60	(NDS)($21C^2 - 12C + 30$)(NP) + P_2 =	43926

[a] C = number of components, NP = number of packing section divisions (NP = 4), NDS = number of data sets, P_1 = 2, P_2 = 6.

Table 6. Estimation Results of Packing-Related Parameters

packing	surface area (m^2/m^3)	void fraction (m^3/m^3)	estimated parameters $\tilde{C}_V$	estimated parameters $\tilde{C}_L$	HETP[25] (m)
Raschig Super-Ring 0.3	315	0.96	0.453	1.550	0.288
Montz-Pak B1-350	350	0.93	0.458	1.246	0.326
Rombopak 9M	320	0.95	0.542	1.482	0.286

$$\boldsymbol{\theta} = \begin{cases} \boldsymbol{\theta_1} = [C_V, C_L]^T \text{ or } F_{SE} & \text{first-layer estimation} \\ \boldsymbol{\theta_2} = [\theta_1, \theta_2, \theta_3, ..., \theta_6]^T & \text{second-layer estimation} \end{cases} \quad (11)$$

The output variables are

$$\mathbf{y}_i = [y_{i,\text{in},1}, y_{i,\text{in},2}, y_{i,\text{in},3}, y_{i,\text{out},1}, y_{i,\text{out},2}, y_{i,\text{out},3}]^T \quad (12)$$

where $y_{i,\text{in}}$ and $y_{i,\text{out}}$ are the vapor molar fractions entering and leaving the packing section in the ith experiment. The input variables are

$$\mathbf{u}_i = \begin{cases} [\varepsilon_i, a_{p,i}, \eta, \Delta P_i, Q_{i,\text{reboiler}}, T_{i,\text{reboiler}}]^T & \text{first-layer estimation} \\ [\varepsilon_i, a_{p,i}, \eta, \Delta P_i, Q_{i,\text{reboiler}}, T_{i,\text{reboiler}}\, \theta_1^T]^T & \text{second-layer estimation} \end{cases} \quad (13)$$

In the second-layer estimation, the estimated packing-related parameters $\boldsymbol{\theta_1}$ are needed as input variables since the flow-related parameters are packing-independent. The covariance matrix $\boldsymbol{\omega}$ of output variables could be specified as

$$\omega_{i,j}^2 = \sigma_{i,j}^2 (y_{i,j}^2 + \zeta)^{\lambda} \quad (14)$$

where $\sigma_{i,j}$ is the constant standard deviation of the measurement error in $\mathbf{y}$ and ζ and λ are coefficients updated automatically by gPROMS in the optimization iterations.

4. Results and Discussion

4.1. Extension of the Billet and Schultes Correlation. As an illustrative example, the Billet and Schultes correlation is extended for three-phase distillation using the hierarchical parameter estimation strategy.

A total number of 150 experimental data sets for the 1-butanol/water/1-propanol system are used in this study. A total of 38 data sets (two-phase distillation) are taken to estimate the packing-related parameters $[C_V, C_L]$, and 60 data sets (three-phase distillation) are used to estimate flow-related parameters $[\theta_1, \theta_2, \theta_3, ..., \theta_6]$. The rest of the data sets are used for validation of the extended correlation.

The parameter estimation turns out to be a large-scale problem. As summarized in Table 5, the estimation problem involves more than 62 000 equality equations in **g** and around 3000 inequality constraints existing in **h** (limitations for temperatures, concentrations, manipulated variables, etc.). When using the hierarchical estimation strategy, the problem is divided into subproblems with a reduced problem dimension. This is one of the benefits of using the hierarchical strategy.

4.1.1. First-Layer Estimation. In the Billet and Schultes correlation, all packing-related contributions to mass transfer are attributed to parameters $[C_V, C_L]$. In this study, the data sets used in estimation are taken from two-phase distillations under various operation conditions (F-factor 0.16−2.55 $\text{Pa}^{0.5}$). The estimated results for all three packings are listed in Table 6.

Taking Raschig Super-Ring 0.3, for example, the values of $[C_V, C_L]$ are available in Billet's work ($C_V = 0.450$, $C_L = 1.500$).[19] The estimated results ($\tilde{C}_V = 0.453$, $\tilde{C}_L = 1.550$) are very close to those in Billet's paper. This confirms that the Billet and Schultes correlation is reliable for two-phase distillation with specified packings.

For Montz-Pak B1-350, the estimated values are $\tilde{C}_V = 0.458$ and $\tilde{C}_L = 1.246$. Since no publication of these parameters is available, they are compared with those of Montz-Pak B1-300 ($C_V = 0.422$, $C_L = 1.165$).[19] This indicates slight enhancements of mass transfer on both the vapor and liquid sides. This is quite reasonable because Montz-Pak B1-350 is expected to have a better mass transfer performance than Montz-Pak B1-300.

Table 7. Estimation Results of Flow-Related Parameters

	estimated parameters[a,b]					
objective function	θ_1	θ_2	θ_3	θ_4	θ_5	θ_6
−1156.85	−0.168	0.790	−0.472	0.781	0.353	0.483
−1153.93	−0.164	0.788	−0.472	0.780	0.216	0.480
−1154.42	−0.165	0.789	−0.471	0.778	0.182	0.486

[a] Limited ranges: $\theta_1 \in [-0.4, -0.05]$, $\theta_2 \in [0.05, 1.5]$, $\theta_3 \in [-0.9, -0.05]$, $\theta_4 \in [0.05, 1.5]$, $\theta_5 \in [0.05, 0.66]$, $\theta_6 \in [0.05, 1.0]$. [b] Initial values: $\theta_1 = -0.2$, $\theta_2 = 0.75$, $\theta_3 = -0.45$, $\theta_4 = 0.75$, $\theta_5 = 0.33$, $\theta_2 = 0.5$.

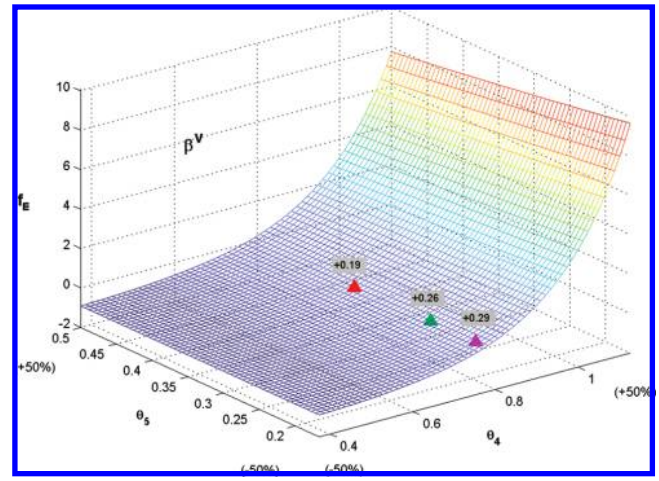

Figure 4. Sensitivity analysis of θ_4 and θ_5 of the function for calculation of vapor-side binary mass transfer coefficients.

For the packing Rombopak 9M, the values of $[C_V, C_L]$ are not available in the literature. Researchers reported that its hydrodynamics is similar to that of gauze packing,[28] while the estimated results ($\tilde{C}_V = 0.542$, $\tilde{C}_L = 1.482$) indicate a much better performance than that of some gauze packings.

As shown in Table 6, Super-Ring 0.3 and Rombopak 9 M have larger $[\tilde{C}_V, \tilde{C}_L]$ than Montz-Pak B1-350. This indicates a larger mass transfer capability and better separation efficiency are expected by using Super-Ring 0.3 and Rombopak 9M. This conclusion agrees well with the experimental HETP measurements for the 1-butanol/water/1-propanol system by Villain.[25] As shown in Table 6, smaller HETP values are suggested to be used for Super-Ring 0.3 and Rombopak 9 M due to their better mass transfer performance.

4.1.2. Second-Layer Estimation. With a large problem dimension, the global optima of the second-layer estimation cannot be guaranteed. In Table 7, results achieved from different estimation runs based on the same initial condition are listed. The deviation between the estimated results (maximum error ±0.004) is in the acceptable error range, indicating good consistency for the estimated parameters, with the exception of θ_5. There are certain deviations in the estimated parameter θ_5. The reason for this is not intuitive, but can be briefly explained by sensitivity analysis. As shown in Table 1, the vapor-side binary mass transfer coefficient can be calculated as $\beta^V = f[(Re_V)^{\theta_4}, (Sc_V)^{\theta_5}]$. The enhancement (±) of β^V by using the new sets of parameters is defined and visualized in Figure 4.

$$f_E = (Re_V)^{\theta_4 - 0.75} (Sc_V)^{\theta_5 - 0.33} - 1 \quad (15)$$

As shown in Figure 4, a +50% change of θ_4 leads to a 10 times bigger β^V, while a 50% change of θ_5 only changes β^V by

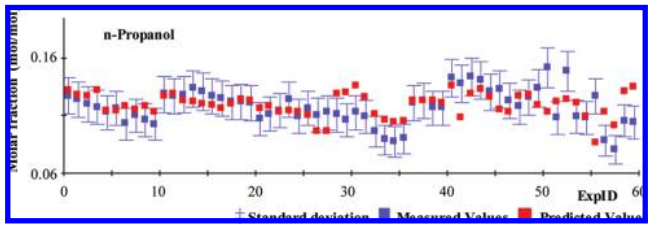

Figure 5. Second-layer estimation results evaluated by standard deviations.

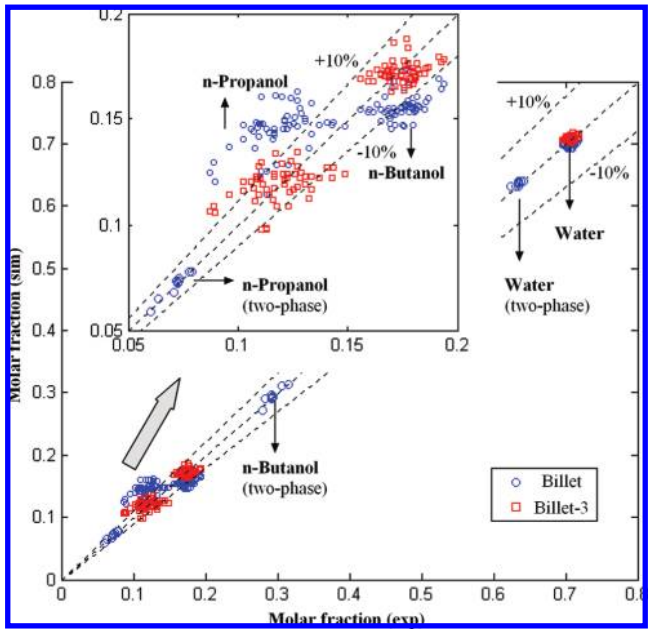

Figure 6. Comparison of experiments with simulations using the original and extended Billet and Schultes correlation concerning the vapor molar fraction of both two-phase and three-phase distillations.

10% (see the ▲ plots for all three sets of estimations). Therefore, in the estimation θ_5 may switch within the limited range but change the objective function (see Table 7) little. This indicates that θ_5 is quite insensitive compared with θ_4. This conclusion also validates for the β^V calculation using the Rocha correlation (and other correlations, e.g., the Onda correlation,[14] Bravo correlation,[16] and Shi and Mersmann correlation[15]). Hence, in the correlation extension, there is no need to adapt (or re-estimate) θ_5. The values of θ_5 are the same as those in the original papers.[19]

To show the reliability of the estimation results, the experimentally measured data, the simulation predictions, and the standard deviations achieved by the estimation are plotted in Figure 5. It can be seen that with the exception of several data sets, the predictions are within the standard deviation limitations.

4.2. Correlation Extension and Prediction Improvement. Using the hierarchical parameter estimation strategy, the Billet and Schultes correlation is extended and can be used for mass transfer calculation in both two-phase and three-phase distillations. In a similar procedure, extension of the Rocha correlation has been successfully carried out. The updated sets of parameters needed in the correlations are summarized in Table 8.

Table 9. SSE Values by Using the Different Correlations for Three-Phase Distillation

	Rocha	Rocha-3	Billet	Billet-3
SSE	0.128	0.026	0.088	0.020

To verify the extended correlation, a comparison of NEQ model simulation results (denoted as "sim") with another 52 (10 two-phase and 42 three-phase) experiments (denoted as "exp") is shown in Figure 6. (1) Concerning two-phase distillation, accurate predictions by using the Billet and Schultes correlation are observed, which validates the reliability of the packing-related parameters [C_V, C_L]. (2) Concerning three-phase distillation, the vapor molar fractions predicted by using the Billet and Schultes correlation have certain deviations. However, by using the extended Billet and Schultes correlation (denoted as "Billet-3"), significant improvements are achieved. The molar fractions predicted by using the extended correlation correspond well with the experimental data, especially for light components 1-propanol and 1-butanol.

To clarify the improvement, a quantitative comparison of the original correlations (Billet, Rocha) and extended correlations (Billet-3, Rocha-3) is made in Table 9. The SSE (sum of squares error) is calculated and evaluated by (NDS = 42) 42 experimental data sets of three-phase distillation:

$$\mathrm{SSE} = \sum_{i=1}^{\mathrm{NDS}} \sum_{j=1}^{C} ((y_{\mathrm{out},i,j} - \tilde{y}_{\mathrm{out},i,j})^2 + (y_{\mathrm{in},i,j} - \tilde{y}_{\mathrm{in},i,j})^2) \tag{16}$$

The SSE values are greatly reduced by using the extended correlations. Though it gives the worst prediction using the Rocha correlation, the extended Rocha correlation (Rocha-3) shows as good a performance as the extended Billet and Schultes correlation (Billet-3). Figure 7 shows the simulated vapor molar fraction for 1-propanol, which also indicates the reliability of the extended correlations. Under high F-factor operations, using the extended Billet and Schultes correlation (Billet-3) can achieve better accuracy since the correlation was originally designed for applications up to the flooding point.

5. Insights into Mass Transfer in Three-Phase Packed Distillation

In the above sections, extension of mass transfer calculation for three-phase distillation in a packed column has been successfully derived and validated. However, there are still some questions to be answered: (1) Does the appearance of the second liquid increase or decrease the overall mass transfer? (2) What causes the primary change in separation efficiency? (3) What

Table 8. Summary of Extensions of Mass Transfer Correlations

	θ_1	θ_2	θ_3	θ_4	θ_5	θ_6	F_{SE} Super-Ring 0.3	F_{SE} Montz-Pak B1-350	F_{SE} Rombopak 9M
Rocha	0.150	0.150	−0.200	0.800	0.333	0.500	–[b]	–	–
Rocha-3[a]	0.158	0.147	−0.187	0.739	0.333	0.277	[0.483]	[0.313]	[0.489]
Billet	−0.200	0.750	−0.450	0.750	0.333	0.500	[0.45, 1.50]	–	–
Billet-3[a]	−0.168	0.790	−0.472	0.781	0.333	0.483	[0.453, 1.55]	[0.458, 1.246]	[0.542, 1.482]

[a] Rocha-3 (extended Rocha correlation) and Billet-3 (extended Billet and Schultes correlation) for three-phase distillation. [b] Not available in the literature.

is the influence of the second liquid on the effective interfacial area and mass transfer coefficient? These questions will be discussed in this section; however, due to the variety of three-phase distillations, all conclusions and remarks are limited to the studied three-phase distillation cases.

5.1. Macroview: Change of the Overall Mass Transfer. The overall mass transfer capacity is regarded as the vapor-phase mass transfer rate of 1-propanol (light component). In the experiments, it can be calculated as

$$\dot{V}_3 = V_{out} y_{out,3} - V_{in} y_{in,3} \tag{17}$$

In the three-phase NEQ model, $\dot{V}_3$ can be computed as

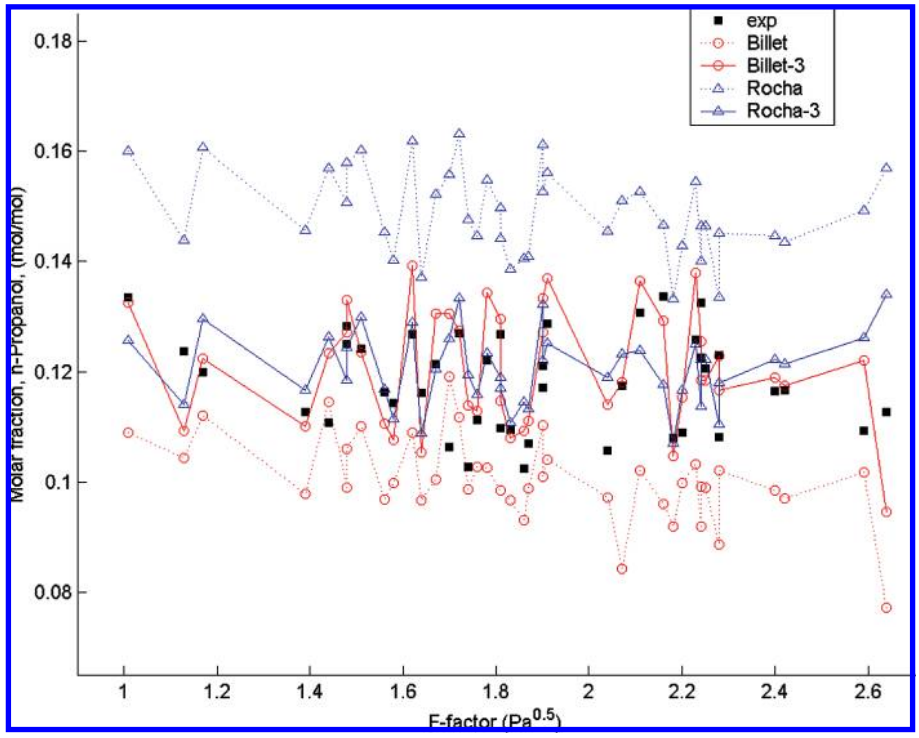

Figure 7. Vapor molar fraction (1-propanol) in three-phase distillations: comparison of prediction results using different correlations.

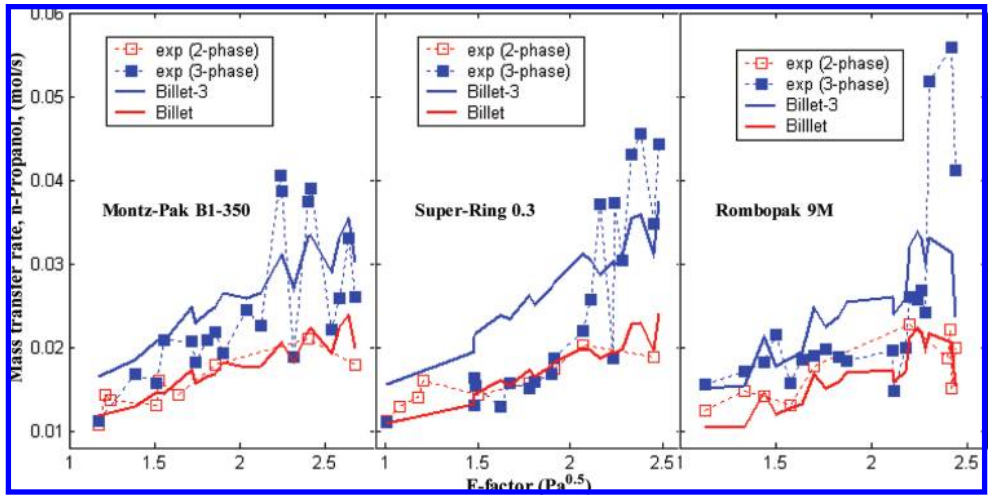

Figure 8. Overall mass transfer capability: comparison of the experimental data and simulated results of two-phase and three-phase distillation.

Table 10. Change of Transfer Variables (Comparison of Three-Phase Distillation with Two-Phase Distillation)

	$\dot{V}$	β^L	β^V			a_e	
Billet-3	↑[a]	↑	↑			↑	
			$(Re_V)^{\theta_4}$ ↑	$(Sc_V)^{\theta_5}$ –	$(Re_L)^{\theta_1}$ ↑	$(We_L)^{\theta_2}$ ↓	$(Fr_L)^{\theta_3}$ ↑
Rocha-3	↑	↑	↓			↑	
			$(Re_V)^{\theta_4}$ ↓	$(Sc_V)^{\theta_5}$ –	$(Re_L)^{\theta_1}$ ↑	$(We_L)^{\theta_2}$ ↓	$(Fr_L)^{\theta_3}$ ↑

[a] Key: ↑, the value increased; ↓, the value decreased.

$$\dot{V}_3 = \sum_{j=1}^{NP} ((N_{j,3}^{V'})a_j^{V'} + (N_{j,3}^{V''})a_j^{V''}) \quad (18)$$

and for two-phase NEQ simulation, it is computed as

$$\dot{V}_3 = \sum_{j=1}^{NP} (N_{j,3}^{V'})a_j^{V'} \quad (19)$$

For both two-phase and three-phase distillations, the experimental results of mass transfer rates according to the *F*-factor are plotted in Figure 8. For a medium *F*-factor (1.0−2.0 $Pa^{0.5}$), the mass transfer rates of three-phase distillation are slightly higher than (or at least the same as) those of two-phase distillation. For a high *F*-factor (2.0−2.7 $Pa^{0.5}$), it is worth noting that there is fluctuation existing in the three-phase distillation results; this may be rooted in differences in the feed concentrations, because we carried out three-phase experiments with feed conditions either rich in water or rich in 1-butanol. However, an overall trend of increasing mass transfer rates in three-phase distillation is observed, which however is not so obvious for two-phase distillation. This indicates that the appearance of the second liquid could enhance the mass transfer in certain distillations.

The simulated mass transfer rates according to the *F*-factor are also plotted in Figure 8 and compared with the experimental data. Billet and Schultes correlation is used in the two-phase NEQ model. The predictions agree well with the experiments. In three-phase distillation simulation, the extended correlation (Billet-3) is used. The predictions show a good tracking ability of the experimental results, especially for high *F*-factor conditions. Though the trace predicted by using Billet-3 cannot catch exactly every experimental point (because the flow-related parameters are estimated on the basis of the overall effect of multiple data sets), it does indicate an enhancement in the overall mass transfer capability in three-phase distillation. The reliability of using the extended mass transfer calculation for three-phase distillation is validated.

The differences in mass transfer ability are directly reflected in the separation efficiency. Experimental investigations of the separation efficiency[23,24] (represented by HTU; the calculation method is available in refs 27, 37, and 38) are depicted in Figure 9. A comparison of the HTU values of 1-propanol for two-phase and three-phase distillations leads to the same conclusion; i.e., for a medium *F*-factor (1.0−2.0 $Pa^{0.5}$), the separation efficiency of three-phase distillation is slightly higher than (or at least the same as) that of two-phase distillation, and for a high *F*-factor (2.0−2.7 $Pa^{0.5}$), an increase in the separation efficiency in three-phase distillation is observed. However, this conclusion may be system-dependent. Even for the same system (1-butanol/water/1-propanol), a decrease in the separation efficiency in three-phase distillation is observed in our previous study[27] for low *F*-factor (0.2−0.6 $Pa^{0.5}$) operations with Sulzer Optiflow C.36.

5.2. Microview: Change of the Transfer Variables. To find the causes for the changed separation efficiency, a thorough analysis of the transfer variables (i.e., $\beta^{V'}$, β'^{V}, $\beta^{V''}$, β''^{V}, $\beta'^{-''}$, and $\beta''^{-'}$ and $a^{V'}$, $a^{V''}$, and $a'^{-''}$) is conducted. An increase in the effective interfacial area a_e (↑) is found in the three-phase distillation simulation. Comparing the estimated values with the original values of parameters [θ_1, θ_2, θ_3] (see Table 8) reveals that the elements $(Re_L)^{\theta_1}$ and $(Fr_L)^{\theta_3}$ increase (↑), which results in an increase in the effective interfacial area a_e. This result is observed when using either the Billet and Schultes correlation or Rocha correlation. Moreover, an increase of the liquid-side

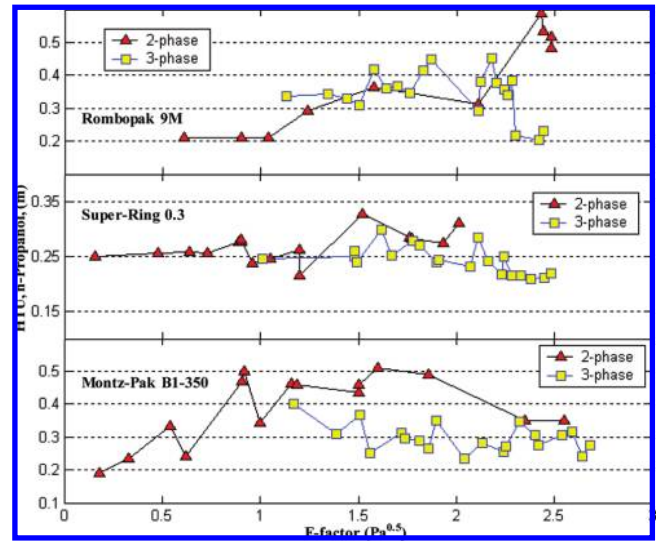

Figure 9. Comparison of the separation efficiency of two-phase and three-phase distillation.[23,24]

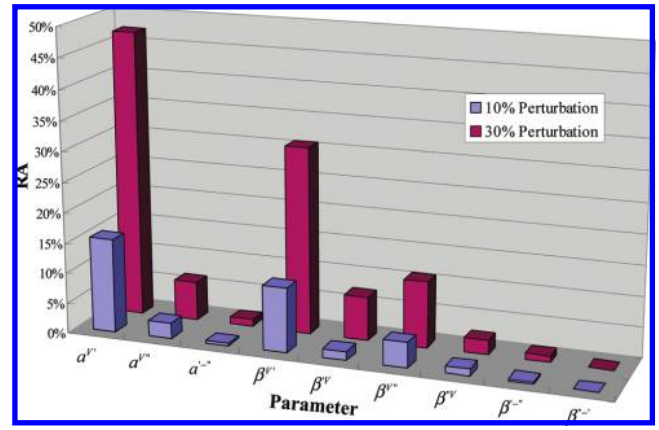

Figure 10. Sensitivity analysis of transfer variables evaluated by the RA using the perturbation test.

binary mass transfer coefficient β^L is found too. The increases of a_e and β^L may be rooted in the change of the liquid velocities. Our previous research on three-phase flows[22,29] reveals that the second liquid can change the liquid flow in a notable way. For the vapor-side binary mass transfer coefficients β^V, the estimations based on the Billet and Schultes correlation and Rocha correlation give contrary results; no deterministic conclusion can be made. However, the mass transfer rates $\dot{V}$ calculated in either case are increased, which agrees well with the plots in Figure 8. More results are given in Table 10.

A further analysis of the sensitivity of the transfer variables suggests that the increase in the effective interfacial area a_e could be the main contribution to the increased separation efficiency. The sensitivity analysis (Figure 10) of the transfer variables is carried out using the perturbation test. The value of each transfer variable is changed by 10% and 30%. For the 1-butanol/water/1-propanol system, 20 different simulation cases are considered using the NEQ model proposed in section 2. The sensitivity is described by the relative error (RA) of the system output (molar fractions):

$$RA = \frac{1}{NDS}\sum_{j=1}^{NDS}\sum_{i=1}^{C}\left(\left|1 - \frac{y_{out,i,j}^{S}}{y_{out,i,j}^{*}}\right| + \left|1 - \frac{y_{in,i,j}^{S}}{y_{in,i,j}^{*}}\right|\right)$$

(y^S, after perturbation; y^*, original molar fraction) (20)

As shown in Figure 10, the effective interfacial area $a^{V'}$ is the most dominant variable. The increase of $a^{V'}$ will surely have a fundamental impact on the mass transfer and should be the main contribution to the increased separation efficiency.

6. Conclusion

This study may serve as the first attempt of developing a reliable mass transfer calculation for three-phase distillation in a packed column. On the basis of our comprehensive research on modeling and experiments, extensions of the Rocha correlation and Billet and Schultes correlation are derived using NEQ model based parameter estimation. To remove the coupling in parameters and to reduce the problem dimension, a hierarchical parameter estimation strategy is proposed. Parameters used in the correlations are classified as packing-related parameters and flow-related parameters, which are estimated using the 98 experimental data sets of two-phase and three-phase distillations, respectively. Correlation validation with another 42 experiments of three-phase distillation and 10 sets of two-phase distillation shows that substantial improvement in the NEQ model accuracy is achieved using the extended correlations. The increased mass transfer capability for the 1-butanol/water/1-propanol system is investigated and explained using the extension of the mass transfer calculation.

In the future, more experimental systems (acetone/toluene/water, acetone/tetrachloroethene/water, cyclohexane/methanol/toluene) will be used in the correlation extensions for three-phase packed distillations. Meanwhile, a theoretical mass transfer model combining both CFD and experimental investigations will be developed for three-phase distillation.

Note Added after ASAP Publication: Minor changes involving selected text in Sections 3.3, 4.1.1, and 4.1.2, as well as Figure 2, have been made to the version of this paper that was published online June 10, 2009. The corected version of this paper was reposted to the Web June 15, 2009.

Acknowledgment

L.C. thanks Technische Universität Berlin for providing him the "Sandwich" DAAD scholarship to pursue further research in Germany. This work is supported by The National Creative Research Groups Science Foundation of China (NCRGSFC; Grant 60721062).

Nomenclature

a = interfacial area [m^2]
a_e = effective interfacial area [m^2/m^3]
a_p = packing specific area [m^2/m^3]
[**B**] = matrix of inverse mass transfer coefficients [s/m]
C = number of components [−]
C_V = vapor-side constant for specific packing [−]
C_L = liquid-side constant for specific packing [−]
$\tilde{C}_V$ = estimated value of C_V [−]
$\tilde{C}_L$ = estimated value of C_L [−]
$\bar{C}$ = molar density [mol/m^3]
d_h = hydraulic diameter [m]
D = binary diffusion coefficient [m^2/s]
E_n = interfacial heat transfer rate [J/s]
F = feed flow rate [mol/s]
f_E = factor of enhancement [−]
F_{SE} = factor for surface enhancement [−]
$\tilde{F}_{SE}$ = estimated value of F_{SE} [−]
Fr = Froude number [−]
g = acceleration due to gravity [m/s^2]
h = liquid holdup [m]
H = enthalpy [J/mol]
J = molar diffusion flux [$mol/(m^2 \cdot s)$]
HETP = height equivalent to that of a theoretical plate [m]
K = phase equilibrium constant [−]
[**k**] = matrix of multicomponent mass transfer coefficients [m/s]
L = liquid flow rate [mol/s]
M = molar mass [kg/kmol]
N = interfacial mass transfer flux [$mol/(m^2 \cdot s)$]
n = number of components in the mixture [−]
NDS = number of data sets [−]
P = pressure [Pa]
Q = heat duty [W]
R = gas constant [$J/(mol \cdot K)$]
Re = Reynolds number [−]
Sc = Schmidt number [−]
T = temperature [K]
V = vapor flow rate [mol/s]
We = Weber number [−]
x = liquid mole fraction [mol/mol]
y = vapor mole fraction [mol/mol]
z = mole fraction [mol/mol]
ΔZ = height of the packing section [m]

Greek Symbols

α = heat transfer coefficient [$J/(m^2 \cdot s \cdot K)$]
β = binary mass transfer coefficient [m/s]
γ = contact angle [deg]
δ = film thickness [m]
ε = packing void fraction [m^3/m^3]
ρ = density [kg/m^3]
η = corrugation angle [deg]
φ = volumetric ratio [−]
$\boldsymbol{\theta}$ = parameters to be estimated [−]
$\boldsymbol{\Phi}$ = objective function [−]
$\boldsymbol{\omega}$ = covariance matrix of output variables [−]
[$\boldsymbol{\Gamma}$] = correction matrix of thermodynamic factors [−]
[$\boldsymbol{\Xi}$] = correction matrix for high flux [−]

Subscripts and Superscripts

F = feed
L = liquid
V = vapor
′ = first liquid phase
″ = second liquid phase
i = component index
j = packing section index
m = component index

Literature Cited

(1) Higler, A.; Chande, R.; Taylor, R.; Baur, R.; Krishna, R. Nonequilibrium Modeling of Three-Phase Distillation. *Comput. Chem. Eng.* **2004**, *28*, 2021.
(2) Block, U.; Hegner, B. Development and Application of a Simulation Model for Three-Phase Distillation. *AIChE J.* **1976**, *22*, 582.
(3) Lao, M.; Taylor, R. Modelling Mass Transfer in Three-Phase Distillation. *Ind. Eng. Chem. Res.* **1994**, *33*, 2637.
(4) Taylor, R.; Krishna, R.; Kooijman, H. Real-World Modeling of Distillation. *Chem. Eng. Prog.* **2003**, *99*, 28.
(5) Cairns, B. P.; Furzer, I. A. Multicomponent Three-Phase Azeotropic Distillation. 1. Extensive Experiment Data and Simulation Results. *Ind. Eng. Chem. Res.* **1990**, *29*, 1349.
(6) Krishnamurthy, R.; Taylor, R. A Nonequilibrium Stage Model of Multicomponent Separation Processes. Part I: Model Description and Method of Solution. *AIChE J.* **1985**, *31*, 449.
(7) Mortaheb, H. R.; Kosuge, H. Simulation and Optimization of Heterogeneous Azeotropic Distillation Process with a Rate-Based Model. *Chem. Eng. Process.* **2004**, *43*, 317.

(8) Eckert, E.; Vanek, T. Some Aspects of Rate-Based Modelling and Simulation of Three-Phase Distillation Columns. *Comput. Chem. Eng.* **2001**, *25*, 603.

(9) Springer, P.; Molen, S.; Krishna, R. The Need for Using Rigorous Rate-Based Models for Simulations of Ternary Azeotropic Distillation. *Comput. Chem. Eng.* **2002**, *26*, 1265.

(10) Saito, N.; Abe, Y.; Kosuge, H.; Asano, K. Homogeneous and Heterogeneous Distillation of Ethanol−Benzene−Water System by Packed Column with Structured Packing. *J. Chem. Eng. Jpn.* **1999**, *32*, 670.

(11) Repke, J.-U.; Villain, O.; Wozny, G. A Nonequilibrium Model for Three-Phase Distillation in a Packed Column: Modelling and Experiments. *Comput. Chem. Eng.* **2004**, *28*, 775.

(12) Repke, J.-U.; Wozny, G. A Short Story of Modelling and Operation of Three-Phase Distillation in Packed Columns. *Ind. Eng. Chem. Res.* **2004**, *43*, 7850.

(13) Taylor, R.; Krishna, R. *Multicomponent Mass Transfer*; John Wiley & Sons: New York, 1993.

(14) Onda, K.; Takeuchi, H.; Okumoto, Y. Mass Transfer Coefficients between Gas and Liquid Phases in Packed Columns. *J. Chem. Eng. Jpn.* **1968**, *1*, 59.

(15) Shi, M. G.; Mersmann, A. Effective Interfacial Area in Packed Column. *Ger. Chem. Eng.* **1985**, *8*, 87.

(16) Bravo, J. L.; Rocha, J. A.; Fair, J. R. Mass Transfer in Gauze Packings. *Hydrocarbon Process.* **1985**, *64*, 91.

(17) Rocha, J. A.; Bravo, J. L.; Fair, J. R. Distillation Columns Containing Structured Packings: A Comprehensive Model for Their Performance. 1. Hydraulic Models. *Ind. Eng. Chem. Res.* **1993**, *32*, 641.

(18) Rocha, J. A.; Bravo, J. L.; Fair, J. R. Distillation Columns Containing Structured Packings: A Comprehensive Model for Their Performance. 2. Mass-Transfer Model. *Ind. Eng. Chem. Res.* **1996**, *35*, 1660.

(19) Billet, R.; Schultes, M. Prediction of Mass Transfer Columns with Dumped and Arranged Packings: Updated Summary of the Calculation Method of Billet & Schultes. *Chem. Eng. Res. Des.* **1999**, *77*, 498.

(20) Olujic, Z. Development of a Complete Simulation Model for Predicting the Hydraulic and Separation Performance of Distillation Columns Equipped with Structured Packings. *Chem. Biochem. Eng. Q.* **1997**, *11*, 31.

(21) Wang, G. Q.; Yuan, X. G.; Yu, K. T. Review Mass Transfer Correlations for Packed Column. *Ind. Eng. Chem. Res.* **2005**, *44*, 8715.

(22) Repke, J.-U.; Ausner, I.; Paschke, S.; Hoffmann, A.; Wozny, G. On the Track to Understanding Three Phases in One Tower. *Chem. Eng. Res. Des.* **2007**, *85*, 1.

(23) Villain, O.; Repke, J.-U.; Wozny, G. Systematic Experimental Investigation of the Three-Phase Distillation. Presented at the 15th International Conference on Process Engingeering & Chemical Plant Design, Cracow, Poland, 2004.

(24) Villain, O.; Repke, J.-U.; Wozny, G. Evaluation of Separation Efficiency of Three-Phase Operated Packed Towers. Presented at the AIChE Spring Meeting, 2005.

(25) Villain, O.; Repke, J.-U.; Wozny, G. Performance Characterization of Three-Phase Operated Column. Presented at the AIChE Annual Meeting, 2003.

(26) Gau, C.-Y.; Stadtherr, M. A. Determine Global Optimisation for Error-in-Variables Parameter Estimation. *AIChE J.* **2002**, *48*, 1192.

(27) Repke, J.-U.; Wozny, G. Experimental Investigations of Three-Phase Distillation in Packed Column. *Chem. Eng. Technol.* **2002**, *25*, 513.

(28) Pelkonen, S. Multicomponent Mass Transfer in Packed Distillation Columns. Ph.D. Thesis, University of Dortmund, Germany, 1997.

(29) Hoffmann, A.; Ausner, I.; Repke, J.-U.; Wozny, G. Fluid Dynamics in Multiphase Distillation Processes in Packed Towers. *Comput. Chem. Eng.* **2005**, *29*, 1433.

(30) Xu, Y.; Paschke, S.; Repke, J.-U.; Wozny, G. Portraying the Countercurrent Flow on Packings by Three-Dimensional Computational Fluid Dynamics Simulations. *Chem. Eng. Technol.* **2008**, *31*, 1445.

(31) Hoffmann, A.; Ausner, I.; Repke, J.-U.; Wozny, G. Detailed Investigation of Multiphase (Gas−Liquid and Gas−Liquid−Liquid) Flow Behavior on Inclined Plates. *Chem. Eng. Res. Des.* **2006**, *84*, 147.

(32) Paschke, S.; Repke, J.-U.; Wozny, G. Untersuchungen von Filmströmungen Mittels Eines Neuartigen Micro Particle Image Velocimetry Messverfahrens. *Chem.-Ing.-Tech.* **2008**, *80*, 1477.

(33) Zavala, V. M.; Biegler, L. T. Large-Scale Parameter Estimation in Low-Density Polyethylene Tubular Reactors. *Ind. Eng. Chem. Res.* **2006**, *45*, 7867.

(34) Zavala, V. M.; Laird, C. D.; Biegler, L. T. Interior-Point Decomposition Approaches for Parallel Solution of Large-Scale Nonlinear Parameter Estimation Problems. *Chem. Eng. Sci.* **2008**, *63*, 4834.

(35) Arora, N.; Biegler, L. T. Parameter Estimation for a Polymerization Reactor Model with a Composite-Step Trust-Region NLP Algorithm. *Ind. Eng. Chem. Res.* **2004**, *43*, 3616.

(36) Faber, R.; Li, P.; Wozny, G. Sequential Parameter Estimation for Large-Scale Systems with Multiple Data Sets. 1. Computational Framework. *Ind. Eng. Chem. Res.* **2003**, *42*, 5850.

(37) Siegert, M. Three-Phase Distillation in Packed Column. *Fortschritt-Berichte VDI Zeitschriften, Reihe 3*; VDI-Verlarg: Düsseldorf, Germany, 1999; No. 586.

(38) Repke, J.-U. Experimental and Theoretical Analysis of Three-Phase Rectification in Packed and Tray Columns. *Fortschritt-Berichte VDI, Reihe 3*; VDI-Verlag: Düsseldorf, Germany, 2002; No. 751.

Received for review March 12, 2009
Revised manuscript received May 20, 2009
Accepted May 27, 2009

IE900404P